

# The valence band alignment at ultrathin SiO<sub>2</sub>/Si interfaces

J. L. Alay

Research Center for Integrated Systems, Hiroshima University, Higashi-Hiroshima 739, Japan

M. Hirose<sup>a)</sup>

Department of Electrical Engineering, Hiroshima University, Higashi-Hiroshima 739, Japan

(Received 7 February 1996; accepted for publication 20 October 1996)

High resolution x-ray photoelectron spectroscopy has been used to determine the valence band alignment at ultrathin SiO<sub>2</sub>/Si interfaces. In the oxide thickness range 1.6–4.4 nm the constant band-offset values of 4.49 and 4.43 eV have been obtained for the dry SiO<sub>2</sub>/Si(100) and the wet SiO<sub>2</sub>/Si(100) interfaces, respectively. The valence band alignment of dry SiO<sub>2</sub>/Si(111) (4.36 eV) is slightly smaller than the case of the dry SiO<sub>2</sub>/Si(100) interface. © 1997 American Institute of Physics. [S0021-8979(97)00203-X]

Ultralarge scale integration (ULSI) of metal-oxide-semiconductor (MOS) devices will need reliable gate oxides thinner than 5.0 nm in the near future. In order to predict the tunneling leakage current through the ultrathin gate oxides, an accurate description of the energy band profile at the ultrathin SiO<sub>2</sub>/Si interfaces or a precise knowledge on the value of the valence band alignment and the conduction band barrier height is required.<sup>1</sup> Although the energy band profile of thick SiO<sub>2</sub>/Si interfaces has been determined by an internal photoemission technique,<sup>2</sup> reliable values for the electron or hole barrier height at ultrathin SiO<sub>2</sub>/Si interfaces remain an unresolved issue. Among the various attempts that have been made in the past to gain a comprehensive understanding of the barrier height or the energy band profile for ultrathin SiO<sub>2</sub>/Si interfaces,<sup>3–8</sup> the consistent picture of the energy band profile has not yet been drawn. Horiguchi and Yoshino<sup>3</sup> have reported that the barrier height for SiO<sub>2</sub>/Si(100) decreases when the oxide thickness becomes thinner than 3.1 nm. On the other hand, by using an electron-beam-assisted scanning tunneling microscopy technique, Heike *et al.*<sup>4</sup> have concluded that the barrier height at the SiO<sub>2</sub>/Si(100) interfaces keeps a constant value of 2.7 eV in the oxide thickness range 1.8–4.5 nm. Grunthaner and Grunthaner<sup>9</sup> have measured valence band spectra of ~6-nm-thick SiO<sub>2</sub> thermally grown on Si(111) by using x-ray photoelectron spectroscopy and found the valence band offset of 4.5 eV. Also, Himpel *et al.*<sup>10</sup> have obtained a valence band alignment of 4.3 eV for the SiO<sub>2</sub>/Si(100) interface by using the Si 2p core level spectrum. Thus well established values of the valence band alignment or the barrier height at ultrathin SiO<sub>2</sub>/Si interfaces are not available.

The purpose of our study is to directly determine the magnitude of the valence band alignment or the hole barrier height at the ultrathin SiO<sub>2</sub>/Si interface and derive a value for the conduction band barrier height by using a measured SiO<sub>2</sub> band gap, based on the valence band density of states (VB-DOS) for ultrathin gate oxides (below 5.0 nm) thermally grown on Si(100) and Si(111) surfaces by employing high-resolution x-ray photoelectron spectroscopy (XPS).

Ultrathin gate oxides were grown at 1000 °C in a 2% dry

O<sub>2</sub> gas diluted with N<sub>2</sub> or at 850 °C in wet ambient. Hydrogen-terminated *p*-type Si(100) substrates (10 Ω cm) were obtained by modified RCA cleaning with a low concentration of NH<sub>4</sub>OH followed by a chemical treatment in a 1% HF solution. The high-resolution XPS measurements were performed with an ESCA-300 (Scientia Instruments AB), using monochromatic Al K $\alpha$  radiation (1486.6 eV) with an acceptance angle of 3.3°. The base pressure during the measurements was maintained in the 10<sup>-10</sup> Torr range. The Si 2p, O 1s, and C 1s core level peaks were measured at photoelectron take-off angles of  $\theta=35^\circ$ , 60°, and 90°, and the valence band spectra were acquired at a take-off angle of 35°. The thicknesses of the ultrathin oxides were evaluated from angle-resolved XPS measurements of the Si 2p core-level by assuming that the Si 2p photoelectron escape depths in Si and SiO<sub>2</sub> are 2.7 and 3.4 nm, respectively.<sup>11</sup>

The deconvolution of the Si 2p core-level peak indicates that the Si<sup>4+</sup> 2p<sub>3/2</sub> peak arising from SiO<sub>2</sub> shifts towards higher binding energies and O 1s also exhibits a similar shift when the oxide thickness increases. The observed peak shift of the Si<sup>0</sup> 2p<sub>3/2</sub> signal from bulk Si is at most 40 meV, whereas the maximum energy shift of Si<sup>4+</sup> 2p<sub>3/2</sub> reaches a value of 333 meV, a factor of 8 larger. A similar result is obtained also for the binding energy of the O 1s core level peak where the maximum energy shift is very close to that of the Si<sup>4+</sup> 2p<sub>3/2</sub> peak. Both dependencies reflect a differential charging effect for core-level peaks originating from the oxide layer and bulk Si. Photoelectrons emitted from the bulk Si are compensated by electrons supplied from the sample holder, while those originated in the ultrathin oxide cannot be fully compensated by tunneling electrons from the substrate. This effect leads to the formation of a positive charge in the oxide layer and the corresponding band bending of SiO<sub>2</sub>. Detailed treatment of this effect has been described in Ref. 12. Once the differential-charging-induced shift for each of the Si 2p components is identified, it is possible to determine the valence band density of states (VB-DOS) with an exact energy scale for ultrathin SiO<sub>2</sub>/Si interfaces as a function of the oxide thickness by means of the XPS valence band spectra. The binding energy corresponding to the O 1s or Si<sup>4+</sup> 2p<sub>3/2</sub> peak for the thinnest (1.6 nm) oxide is taken as the energy reference for all other oxides since the charging effect is minimum or negligible for this oxide. Therefore, the

<sup>a)</sup>Electronic mail: hirose@sxsys.hiroshima-u.ac.jp

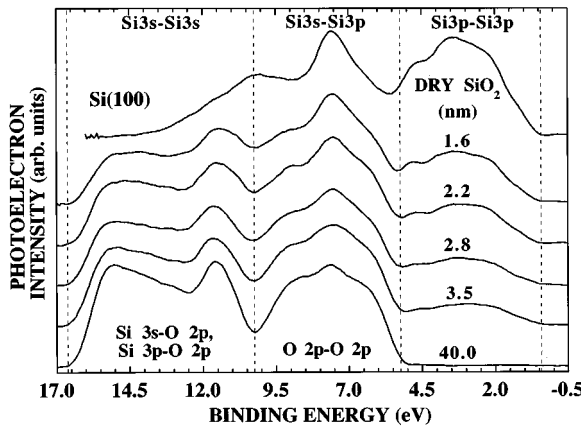


FIG. 1. Valence band density of states for ultrathin dry  $\text{SiO}_2/\text{Si}(100)$  interfaces obtained by high-resolution XPS. The VBDOS for a H-terminated Si surface and a 40.0-nm-thick dry  $\text{SiO}_2$  layer are also displayed for comparison. The charging effect has been corrected for all spectra.

oxide valence band edge energies have been corrected by shifting each spectrum by the value given by the difference between the respective O 1s or  $\text{Si}^{4+}$   $2p_{3/2}$  peak position and that of the 1.6 nm oxide to correct the oxide charging contribution.

The VBDOS measured for the 1.6-, 2.2-, 2.8-, and 3.5-nm-thick dry  $\text{SiO}_2/\text{Si}(100)$  are shown in Fig. 1. The VBDOS of the H-terminated  $\text{Si}(100)$  and a 40-nm-thick dry  $\text{SiO}_2$  are also displayed as references in the same figure, showing that the VBDOS of the various ultrathin dry  $\text{SiO}_2/\text{Si}(100)$  can be considered as a linear combination of the  $\text{Si}(100)$  and  $\text{SiO}_2$  VBDOS spectra. The method employed here to obtain the ultrathin  $\text{SiO}_2$  VBDOS depicted of any Si substrate influence consists of subtracting the Si substrate VBDOS component, which has been measured from a hydrogen-terminated  $p\text{-Si}(100)$  sample, from the measured  $\text{SiO}_2/\text{Si}$  interface VBDOS.

The ultrathin and thick dry oxide VBDOS show nearly identical spectra as shown in Fig. 2. Note that the top of the valence band of the various ultrathin oxides coincides with that of the thick oxide when the differential charging effect

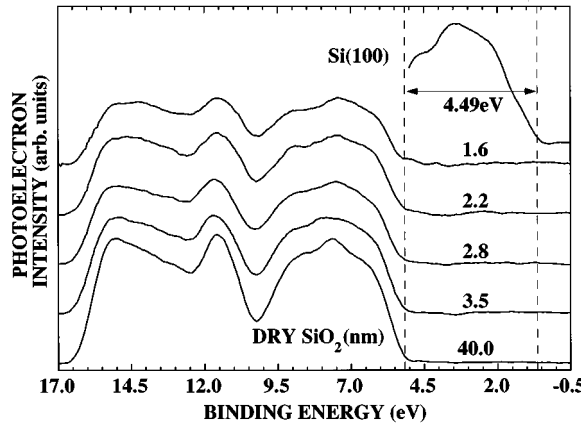


FIG. 2. Valence band density of states for ultrathin dry oxides after having subtracted the Si substrate component. The charging effect has been corrected for all spectra.

TABLE I. Valence band alignment or hole barrier height and electron barrier height for the various ultrathin  $\text{SiO}_2/\text{Si}$  interfaces.

	Valence band alignment (eV)	Conduction band barrier height (eV)
dry $\text{SiO}_2/\text{Si}(100)$	4.49	3.29
wet $\text{SiO}_2/\text{Si}(100)$	4.43	3.35
dry $\text{SiO}_2/\text{Si}(111)$	4.36	3.42

of oxides is carefully corrected. The difference between the energy position of the top of the ultrathin  $\text{SiO}_2$  valence band and the top of the  $\text{Si}(100)$  reference valence band was determined by the method described in Ref. 9, yielding the valence band alignment, which is a constant value of 4.49 eV regardless of the oxide thickness from 1.6 to 3.5 nm. An  $\text{SiO}_2$  band gap of 8.90 eV as recently obtained for ultrathin gate oxides by the analysis of the O 1s plasmon loss peak<sup>13</sup> can yield the corresponding conduction band barrier height of 3.29 eV for ultrathin dry  $\text{SiO}_2/\text{Si}(100)$  interfaces. In the case of wet oxides we have obtained similar VBDOS with a constant valence band alignment value of 4.43 eV regardless of the oxide thickness from 2.5 to 4.4 nm and a corresponding electron barrier height of 3.35 eV. Thus determined valence band alignment and the conduction band barrier height of dry  $\text{SiO}_2/\text{Si}(100)$  have been used to calculate the tunneling current through 3–5-nm-thick gate oxides. It is demonstrated that the measured tunnel current density versus oxide voltage characteristic agrees well with the calculated results.<sup>1</sup>

The values found for the valence band alignment and the conduction band barrier height are summarized in Table I for the various ultrathin  $\text{SiO}_2/\text{Si}$  interfaces. The reported value of the conduction band barrier height for thick  $\text{SiO}_2/\text{Si}(100)$  is known to be 3.25 eV (see Ref. 14) that is close to the value obtained for ultrathin  $\text{SiO}_2/\text{Si}(100)$ . It is interesting to note that the value of the valence band alignment for dry  $\text{SiO}_2/\text{Si}(100)$  is 0.13 eV larger than dry  $\text{SiO}_2/\text{Si}(111)$ . Although this difference is not far from the experimental error bar of 0.1 eV, this reproducible result implies that the band alignment depends slightly on the silicon surface orientation. A possible mechanism to explain this might be the existence of strained Si–O–Si bonds near the  $\text{SiO}_2/\text{Si}$  interface. In fact, it is shown that the LO-phonon peak of ultrathin  $\text{SiO}_2$  on  $\text{Si}(111)$  exhibits a larger redshift than that for  $\text{SiO}_2/\text{Si}(100)$ .<sup>15</sup> The redshift is largest at the interface and becomes small in the oxide layer within 2 nm from the interface. Since the redshift is explained by compressive stress in the oxide, the higher stress is existing in the  $\text{SiO}_2/\text{Si}(111)$  interface as compared to  $\text{SiO}_2/\text{Si}(100)$ . Such orientation dependent stress in the interface might modify the interface dipole moment for the  $\text{SiO}_2/\text{Si}(111)$  and  $\text{SiO}_2/\text{Si}(100)$  boundaries.

In summary, the VBDOS of ultrathin oxides grown on Si is found to be nearly identical to that of thick  $\text{SiO}_2$ . The valence band alignment of 4.49 eV for the dry  $\text{SiO}_2/\text{Si}(100)$  interfaces is very close to the wet  $\text{SiO}_2/\text{Si}(100)$  value (4.43 eV). The measured values are constant regardless of the oxide thickness from 1.6 to ∼5.0 nm. A little difference in the valence band alignment or conduction band barrier height

between  $\text{SiO}_2/\text{Si}(100)$  and  $\text{SiO}_2/\text{Si}(111)$  interfaces could be associated with different built-in strain between  $\text{SiO}_2/\text{Si}(100)$  and  $\text{SiO}_2/\text{Si}(111)$  interfaces.

The authors would like to acknowledge M. Fukuda and T. Yoshida at the Department of Electrical Engineering, T. Kugimiya and Professor S. Yokoyama at the Research Center for Integrated Systems for their assistance in this work.

<sup>1</sup>T. Yoshida, D. Imafuku, J. Alay, S. Miyazaki, and M. Hirose, *Jpn. J. Appl. Phys.* **34**, 903 (1995).

<sup>2</sup>P. V. Dressendorfer and R. C. Barker, *Appl. Phys. Lett.* **36**, 933 (1980).

<sup>3</sup>S. Horiguchi and H. Yoshino, *J. Appl. Phys.* **58**, 1597 (1985).

<sup>4</sup>S. Heike, Y. Wada, S. Kondo, M. Lutwyche, K. Murayama, and H. Kuroda, *Extended Abstracts of the International Conference on Solid State Devices and Materials*, Yokohama, 1994 (Business Center for Academic Societies Japan, Tokyo, 1994), p. 40.

<sup>5</sup>L. A. Kasprzak, R. B. Laibowitz, and M. Ohring, *J. Appl. Phys.* **48**, 4281 (1977).

<sup>6</sup>H. C. Card, *Solid State Commun.* **14**, 1011 (1974).

<sup>7</sup>G. Lewicki and J. Maserjian, *J. Appl. Phys.* **46**, 3032 (1975).

<sup>8</sup>V. Kumar and W. E. Dahlke, *Solid-State Electron.* **20**, 143 (1977).

<sup>9</sup>F. J. Grunthaner and P. J. Grunthaner, *Mater. Sci. Rep.* **1**, 147 (1986).

<sup>10</sup>F. J. Himpsel, F. R. McFeely, A. Taleb-Ibrahimi, and J. A. Yarmoff, *Phys. Rev. B* **38**, 6084 (1988).

<sup>11</sup>N. Terada, T. Haga, N. Miyata, K. Moriki, M. Fujisawa, M. Morita, T. Ohmi, and T. Hattori, *Phys. Rev. B* **46**, 2312 (1992).

<sup>12</sup>J. L. Alay, M. Fukuda, C. H. Bjorkman, K. Nakagawa, S. Yokoyama, S. Sasaki, and M. Hirose, *Jpn. J. Appl. Phys.* **34B**, 653 (1995).

<sup>13</sup>S. Miyazaki, H. Nishimura, M. Fukuda, L. Ley, and J. Ristin, *Appl. Surf. Sci.* (to be published).

<sup>14</sup>S. M. Sze, *Physics of Semiconductor Devices* (Wiley, New York, 1969), Chap. 9.

<sup>15</sup>T. Yamazaki, C. H. Bjorkman, S. Miyazaki, and M. Hirose, in *Proceedings of the 22nd International Conference on The Physics of Semiconductors*, 1994, Vol. 3, p. 2653.